# Self-cleaning of superhydrophobic surfaces by self-propelled jumping condensate

Katrina M. Wisdom[a,1], Jolanta A. Watson[b,1], Xiaopeng Qu[a,1], Fangjie Liu[a], Gregory S. Watson[b,2], and Chuan-Hua Chen[a,2]

[a]Department of Mechanical Engineering and Materials Science, Duke University, Durham, NC 27708; and [b]School of Marine and Tropical Biology, James Cook University, Townsville, QLD 4811, Australia

Edited by Xiao Cheng Zeng, University of Nebraska, Lincoln, NE, and accepted by the Editorial Board April 2, 2013 (received for review June 24, 2012)

**The self-cleaning function of superhydrophobic surfaces is conventionally attributed to the removal of contaminating particles by impacting or rolling water droplets, which implies the action of external forces such as gravity. Here, we demonstrate a unique self-cleaning mechanism whereby the contaminated superhydrophobic surface is exposed to condensing water vapor, and the contaminants are autonomously removed by the self-propelled jumping motion of the resulting liquid condensate, which partially covers or fully encloses the contaminating particles. The jumping motion off the superhydrophobic surface is powered by the surface energy released upon coalescence of the condensed water phase around the contaminants. The jumping-condensate mechanism is shown to spontaneously clean superhydrophobic cicada wings, where the contaminating particles cannot be removed by gravity, wing vibration, or wind flow. Our findings offer insights for the development of self-cleaning materials.**

particle adhesion and removal | water-repellant insect wings | nanostructured interfaces | capillary forces

Both natural and synthetic superhydrophobic surfaces are believed to achieve self-cleaning by the so-called "lotus effect" (1, 2). The lotus effect typically refers to the removal of the contaminating particles by impacting and/or rolling water droplets (1, 3). The superhydrophobicity is important because of the associated large contact angle and small hysteresis (4), which promotes the rolling motion carrying away contaminants. According to the conventional wisdom of the lotus effect, the self-cleaning function will cease without incoming droplets or favorable external forces, posing severe restrictions for practical applications of superhydrophobic materials.

Here, we demonstrate an autonomous mechanism to achieve self-cleaning on superhydrophobic surfaces, where the contaminants are removed by self-propelled jumping condensate powered by surface energy. When exposed to condensing water vapor, the contaminating particles are either fully enclosed or partially covered with the resulting liquid condensate. Building upon our previous publications showing self-propelled jumping upon drop coalescence (5, 6), we show particle removal by the merged condensate drop with a size comparable to or larger than that of the contaminating particle(s). Further, we report a distinct jumping mechanism upon particle aggregation, without a condensate drop of comparable size to that of the particles, where a group of particles exposed to water condensate clusters together by capillarity and self-propels away from the superhydrophobic surface.

The jumping-condensate mechanism reported here offers a unique route toward self-cleaning, with potential applications ranging from microelectronic wafer cleaning to heat exchanger maintenance (7). Particle removal is often accomplished in a gas flow or a liquid stream by hydrodynamic shear stresses, which are parallel to the surface. The parallel hydrodynamic forces are not ideal in competing against the adhesive mechanisms such as van der Waals forces, which are predominantly perpendicular to the surface (7–9). In this regard, the out-of-plane directionality of the jumping-condensate removal mechanism is particularly effective in dislodging adhered particles.

The cicada wing is used as a model superhydrophobic surface. Most cicadas as well as other "large-winged" insects have extremities that are too short to actively clean the wings (10), but are exposed to a multitude of contaminants, including soil fragments, industrial dusts, plant pollen, and pathogenic microorganisms (e.g., bacteria) (1, 10, 11). For these insects, self-cleaning is important to preserve wing functionalities such as those involving flight and antireflection (10, 12–14). Although self-cleaning can be accomplished on the wings with the lotus effect (10), rain may not be available for prolonged periods of time and, in extreme circumstances, may be absent during the short life span (12) of an insect. On the other hand, many insects live in a humid environment in which condensation of atmospheric vapor takes place on a daily basis. We show that the jumping condensate occurring during vapor condensation is highly effective in removing both pollen and silica particles on cicada wings. When other removal mechanisms are ineffective or absent, the jumping-condensate mechanism is expected to achieve self-cleaning on a variety of superhydrophobic surfaces, including water-repellent plant leaves, insect wings, and synthetic materials.

## Particle Removal Processes by Jumping Condensate

The nanostructured cicada wing (Fig. 1) is a model superhydrophobic surface on which liquid condensate can spontaneously jump upon coalescence. We first show how different jumping processes carry away particles that are initially adhering to the wing surface.

**Model Surfaces and Particles.** A photograph of the cicada (*Psaltoda claripennis*) is shown in Fig. 1*A*. The forewings of the insect are typically 34–42 mm in length with green veins along the leading edge. The cicada wings are superhydrophobic because the wing cuticle consists of arrays of conical protuberances covered with a hydrophobic wax layer (Fig. 1*B*). The protuberances are spherically capped and hexagonally arranged, with a spacing and height of ~200 nm and a radius of curvature at the apex in the range of 25–45 nm. The apparent contact angle of water on the nanostructured membrane was between 148° and 168°, depending on the location. The nanostructural features are present on all areas of the dorsal and ventral membrane sections on both the hind wings and the forewings. Similar features have been noted on the wings of a number of other cicada species (11, 13).

Two types of particles were used to approximate the wettability of the less hydrophilic plant matter and more hydrophilic

Author contributions: G.S.W. and C.-H.C. designed research; K.M.W., J.A.W., X.Q., and F.L. performed research; K.M.W., J.A.W., X.Q., F.L., G.S.W., and C.-H.C. analyzed data; and C.-H.C. wrote the paper.

The authors declare no conflict of interest.

This article is a PNAS Direct Submission. X.Z. is a guest editor invited by the Editorial Board.

[1]K.M.W., J.A.W. and X.Q. contributed equally to this work.

[2]To whom correspondence may be addressed. E-mail: chuanhua.chen@duke.edu or gregory.watson1@jcu.edu.au.

This article contains supporting information online at www.pnas.org/lookup/suppl/doi:10.1073/pnas.1210770110/-/DCSupplemental.

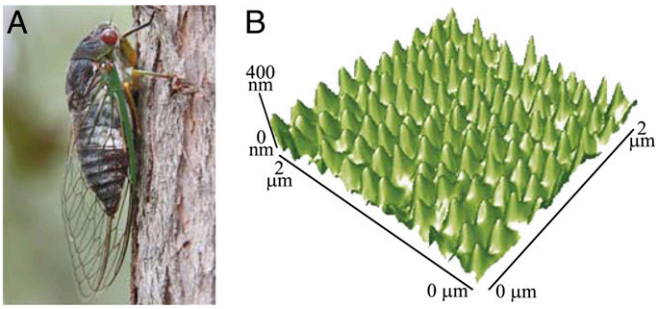


**Fig. 1.** Superhydrophobic cicada wing. (*A*) The cicada is usually oriented skyward when at rest. (*B*) The wing is superhydrophobic because of the nanostructured surface shown by an atomic force microscope (AFM) image.

soil fragments. The silver-coated glass particles had a water contact angle of ~10° and a nominal diameter of 50 μm, and the polymethyl methacrylate (PMMA) particles had a contact angle of ~60° and a diameter of 100 μm. The relatively large particles were used to facilitate the visualization of the particle removal process. To show the negligible effects of gravitational removal, the superhydrophobic wings were oriented vertically throughout this section. These particles were not removed by gravity unless they were carried away by very large drops with a diameter approaching the millimetric capillary length. Note that the images in Figs. 2–4 were rotated to more clearly show the jumping process, with gravity pointing rightward.

**Particle Removal Processes.** When the superhydrophobic cicada wing was subjected to a condensing vapor flow, water vapor condensed on the surface of the wing and the adhering particles. The interaction of the resulting liquid condensate and the particles on the superhydrophobic surface could lead to autonomous cleaning of the particles. The particle removal process by the jumping water condensate was strongly influenced by the wettability. Depending on their wettability, particles have a tendency to either attach to the air–liquid interface or detach into the bulk fluid. As a guideline, the energy required to detach a spherical particle from a flat interface is proportional to $(1-|\cos\ \theta_1|)^2$, where $\theta_1$ is the contact angle of water on the particle (15). Three different processes of particle removal were identified: floating, lifting, and aggregating.

***Floating removal.*** In Fig. 2, the glass particle was first entrained by a growing condensate drop that detached the particle from the superhydrophobic surface. The condensate drop enclosing the particle subsequently jumped away from the surface upon merging with neighboring drop(s). The floating removal process was most easily demonstrated with very hydrophilic particles because of the low energy barrier to detach a particle from the air–liquid interface to the bulk liquid.

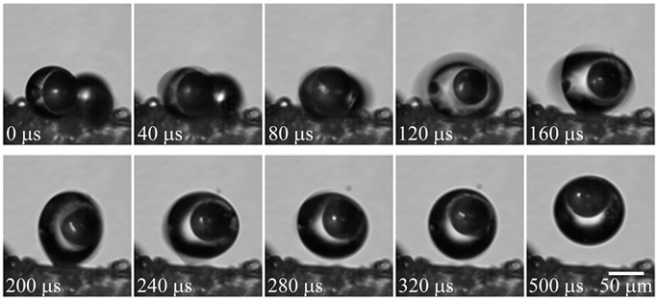


**Fig. 2.** Floating removal process: A 50-μm-diameter glass particle was initially floated inside a condensate drop. When this drop coalesced with a neighboring drop, the capillary-inertial oscillation of the merged drop interacted with the superhydrophobic wing surface, resulting in an out-of-plane jumping drop that carried away the floated particle. For the cascading coalescence processes leading to the configuration at 0 μs, see Movie S1.

With floating removal, the particle detachment from the superhydrophobic surface occurred before any jumping motion. The actual removal process should be similar to that in earlier reports of particle removal by the passage of a liquid–gas phase boundary (16, 17). The adhesive force between the particle and the rising liquid–gas interface of a growing condensate drop scales as the capillary force (16, 17),

$$f_c \sim \sigma R_p, \qquad [1]$$

where $\sigma$ is the surface tension and $R_p$ is the particle radius. The more wettable particle will experience a stronger floating force but the $R_p$ scaling remains the same.

For the floating mechanism in Fig. 2, the floated particle was eventually carried away by the jumping condensate drops upon coalescence. As detailed in our earlier paper (5), the jumping motion in Fig. 2 resulted from the surface energy released upon drop coalescence. The capillary-inertial oscillation processes were apparent in Fig. 2, where the merged drop alternated between oblate and prolate configurations. The large apparent contact angle associated with the superhydrophobic surface was important because drop coalescence occurred above the substrate, allowing the rapidly expanding liquid bridge between the merging drops to impact the substrate (6). During the transition from the oblate shape (Fig. 2, 40 μs) to the prolate one (160 μs), the capillary-inertial impingement process gave rise to a counterforce from the surface, propelling the merged drop to jump perpendicularly (5).

***Lifting removal.*** In Fig. 3, a less hydrophilic particle with a contact angle of 60° was used, and the particle was only partially covered with a "cap" of condensate. The condensate drop partially capping the particle coalesced with neighboring drops, leading to the jumping motion of the merged drop that subsequently pulled the particle away from the surface. Despite similar capillary-inertial processes leading to the jumping drops in Figs. 2 and 3, a fundamental difference existed in the actual particle removal process. Unlike in Fig. 2 where the particle was dislodged from the surface before the jumping motion, the particle in Fig. 3 was lifted away from the surface by the merged drop after its jumping motion. Although the lifting processes could in principle occur for any particle with a nonzero contact angle, it was much more common to observe the lifting process on the less hydrophilic PMMA particles because of the higher energy barrier for the water drop to completely enclose these particles.

The lifting force exerted on the particle by the jumping drop is also a consequence of the liquid–gas phase boundary and should follow the capillary force scaling in Eq. **1**, $f_c \sim \sigma R_p$. Such a force can be provided by the momentum of the merged drop with a jumping velocity scaling as $v_{ci} \sim \sqrt{\sigma/(\rho R_d)}$, where $\rho$ is the liquid density and $R_d$ is the drop radius (5). With processes governed by the capillary-inertial timescale, $t_{ci} \sim \sqrt{\rho R_d^3/\sigma}$, the available force scales as

$$f_{ci} \sim \sigma R_d \gtrsim \sigma R_p \sim f_c, \qquad [2]$$

because the drop radius ($R_d$) is typically larger but of the same order as the particle radius ($R_p$). Note that the capillary-inertial force ($f_{ci}$ in Eq. **2**) due to drop coalescence has a dynamic origin (5), whereas the capillary force due to gradually rising liquid–gas interface ($f_c$ in Eq. **1**) has a quasi-static origin (16, 17).

***Aggregating removal.*** Unlike the floating and lifting mechanisms in Figs. 2 and 3, respectively, the particle removal in Fig. 4 is no longer preceded by the capillary-inertial oscillation of condensate drops with a size comparable to (or larger than) that of the

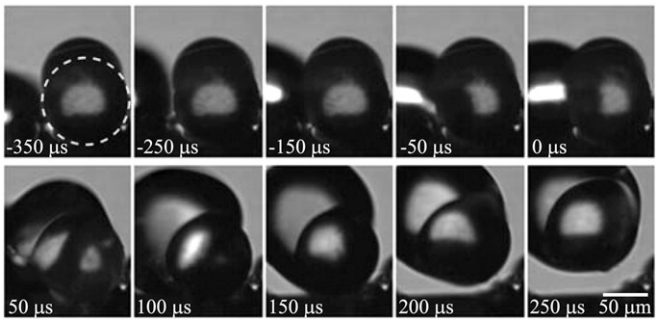


**Fig. 3.** Lifting removal process: A 100-μm-diameter PMMA particle indicated by the dashed circle was partially capped with some water condensate. The capping water film coalesced with an approaching drop at 0 μs, triggering the jumping of the merged drop. The jumping drop lifted away the particle that remained on the wing surface until 200 μs. The approaching drop was the result of a previous coalescence; see details in Movie S2.

particles. In this sense, the aggregating removal mechanism is fundamentally different even though it is still driven by surface energy. When a clump of particles was subject to condensing vapor, the water condensate formed liquid bridges among neighboring particles. Under the right circumstances as in Fig. 4, the immersion force among neighboring particles (18) deformed the loosely connected particles into a tighter cluster, and the particle cluster eventually jumped away from the surface. The aggregating mechanism appeared to be sensitive to the particular arrangement of the particle clump and was observed much less frequently compared with the floating and lifting mechanisms.

The aggregating mechanism of particle removal seems to be unique to the superhydrophobic surface, which among other things minimizes the adhesion between the particle cluster and the surface. Although the detailed mechanism of this multibody aggregation process is beyond the scope of the present paper, the aggregating and subsequent jumping process can be appreciated from an energetic point of view. The aggregation process reduced the overall surface area, releasing surface energy that was converted to kinetic energy of the jumping particle cluster. Because the particle cluster is held together by the capillary forces, the force available to dislodge an individual particle should still scale as the capillary force as in Eq. **1**, $f_c \sim \sigma R_p$.

**Discussion.** For all three removal mechanisms, the timescale for the jumping-condensate processes is very short (typically submilliseconds), which is consistent with the capillary-inertial scaling ($t_{ci}$). The short timescale implies the sudden release of the surface energy that has accumulated during a much longer condensation process, which is crucial for producing a large power density required for the jumping condensate to carry payloads and achieve self-cleaning. In this sense, the jumping-condensate cleaning process is similar to the ballistospore discharge processes (19, 20).

The capillary-inertial scaling was developed for the coalescence of drops with the same radius. For coalescence of drops of comparable size, the capillary-inertial scaling with an average drop radius is a good first approximation. When the drop radii are significantly different, these scaling laws are no longer appropriate. As a matter of fact, coalescence of drops of disparate radii does not always result in jumping from the superhydrophobic surface (21), likely due to the small yet finite adhesion between the superhydrophobic surface and the drops (especially the larger drop). However, cascading coalescence processes will ensure that the larger condensate drops merge with sufficiently large drops sooner or later. See, for example, movie S2 in ref. 5: On a horizontally held superhydrophobic substrate cooled below the dew point, while larger condensate drops tended to stay in the field of view for longer, each condensate drop eventually disappeared by the jumping process. In addition, the really large drops are also easily removed by external forces such as gravity and wind. The force scaling for the asymmetric drop coalescence warrants further study. We note that the capillary-inertial force scaling, $f_{ci} \sim \sigma R_d$, has also been adopted with some experimental support in the ballistospore literature (20), where the asymmetric coalescence is between a spherical (Buller's) drop (22) with a radius $R_d$ and an irregularly shaped and partially wetted spore.

## Self-Cleaning by Jumping Condensate

In the previous section, we showed that particles adhering to superhydrophobic surfaces can be autonomously removed by the jumping condensate. Despite differences in the detailed processes for floating, lifting, and aggregating removal, each mechanism is driven by capillarity and can therefore provide a removal force on the order of the capillary force, $f_c \sim \sigma R_p$. We now show that the jumping-condensate removal mechanism is sufficient and effective in achieving the self-cleaning function.

**Adhesive and Dislodging Forces.** As a model system, we consider the force required to detach a rigid spherical particle of radius $R_p$ from a flat substrate (7). The edge-to-edge separation of the particle from the substrate is $S$. The attractive forces include the van der Waals force (8, 9),

$$f_w \sim -\left(A_H/S^2\right)R_p, \qquad [3]$$

where $A_H$ is the Hamaker constant. If there is a liquid bridge between the particle and the substrate, e.g., due to capillary condensation of water vapor, the capillary force also contributes to the attraction. For a static liquid bridge, the capillary bridging force is maximum when $S = 0$ (8, 9),

$$f_b \sim -\sigma(\cos\theta_1 + \cos\theta_2)R_p, \qquad [4]$$

where $\theta_1$ and $\theta_2$ are the contact angles of the liquid with the particle and the substrate, respectively. Note that for hydrophobic surfaces, the capillary bridging may be through a gas bubble instead of a liquid column (23), and the gas bubble naturally exists on textured superhydrophobic surfaces. Both the van der Waals force and the static capillary force are linearly proportional to the particle radius. Although these scaling relations are based on flat surfaces, the surface roughness on the wing will not likely change the power-law dependence on the particle radius.

A dislodging mechanism is needed to overcome the attractive force of van der Waals and capillary origins, both scaling as $f_w, f_b \sim R_p$. Among the possible dislodging mechanisms (7), Columbic repulsion is unlikely to yield consistent repulsive forces for all contaminants, because the contaminating particles can be neutral

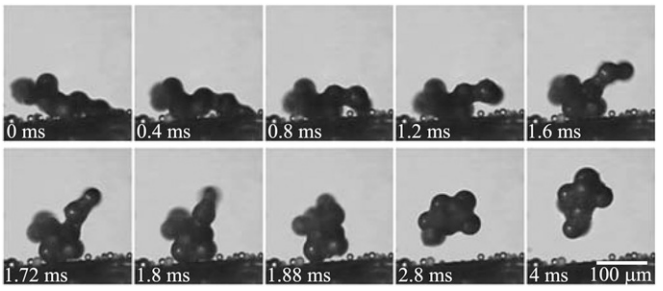


**Fig. 4.** Aggregating removal process: When water vapor condensed on a clump of 50-μm-diameter glass particles, the growing liquid bridge among the neighboring drops led to particle aggregation. The aggregation process caused the particle clump to eventually jump off the surface (Movie S3).

or charged to either polarity. Gravitational and inertial forces are proportional to the particle mass,

$$f_i \sim \rho_p a R_p^3, \quad [5]$$

where $\rho_p$ is the density of the particle, and $a$ is the acceleration owing to gravitational, centrifugal, or vibrational forces. The $R_p^3$ scaling is unfavorable for removing fine particles. Hydrodynamic shear force is another potential removal mechanism. For a particle subjected to a linear velocity gradient with a shear rate of $\dot{\gamma}$, which is a reasonable assumption for a small particle well within the viscous boundary layer near the substrate, the shear force scales as (9)

$$f_s \sim \eta \dot{\gamma} R_p^2, \quad [6]$$

where $\eta$ is the viscosity of the surrounding fluid. Because of the $R_p^2$ scaling, the hydrodynamic removal mechanism is unfavorable for small particles, particularly when the surrounding medium is air with a low viscosity. Because rain is not always present, the shear force mechanism can be unreliable for the vital task of self-cleaning. It should be noted that the hydrodynamic shear force is perpendicular to the aforementioned attractive forces and may therefore lead to particle removal by gradual peeling, which requires much less force than instantaneous separation (8).

In the previous section, we showed that the jumping-condensate removal mechanisms exhibit the right scaling trends with respect to the particle radius with $f_c, f_{ci} \sim \sigma R_p$. The only prerequisite is the condensation of water vapor, which is very common in the summer when insects are most abundant. The presence of water condensate has the added advantage of lowering the Hamaker constant and therefore the van der Waals force, typically by an order of magnitude (8, 9).

**Jumping Condensate vs. Other Cleaning Mechanisms.** According to the above analysis of the mechanisms for dislodging and removing fine particles, the jumping-condensate removing mechanism should be much more effective than other mechanisms such as vibrational force and wind shear, which is shown in Fig. 5. Spherical particles 8 μm in diameter were first scattered on the cicada wing (Fig. 5*A*) and then mechanically vibrated on a stage (Fig. 5*B*). The vibration frequency was 22 Hz, around the natural flapping frequency of cicada wings (24); the peak-to-peak amplitude was 7 mm, corresponding to a maximum velocity of 0.5 m/s. Although this velocity was only 1/10th that at the tip of a flapping cicada wing, the result suggested that vibration alone cannot achieve self-cleaning because the portion of the wing closer to the hinge will always experience a smaller vibration velocity. See Fig. S1 for a more rigorous proof of the negligible effects of wing vibration, where the flapping motion of the cicada wing was closely simulated.

The particle-laden wing was then subjected to airflow in a wind tunnel at 8 m/s, close to the global average wind speed (25) to simulate a typical environment. In the wind flow, the particles remain adhered to the wing (Fig. 5*C*). Note that depending on how the particles were deposited, some particles were easily removed by wind, whereas others would remain stuck to the wing at a speed of up to 12 m/s (the highest velocity achievable with our setup). The variability is a consequence of the possibility of a gradual lateral removal of the particles by shear forces, depending on how specific particles adhere to the wing. In Fig. 5*C*, for example, some particles were slightly dislocated by the wind, but none were removed.

When the same wing was subjected to vapor condensation for a few minutes, the particles adhering to the surface under wind were dislodged. The three-particle cluster in the center of Fig. 5*C* was dislodged to a new location in Fig. 5*D*. A series of jumping events led to the displacement of the particle cluster. A representative dislodging process on the horizontally held wing is shown in Fig. 5*E*, where the drop laden with the same particle cluster merged with an approaching droplet (Fig. 5*E*, 0 ms) and jumped up into the air upon coalescence. Because of the out-of-plane jumping, the merged drop became out of focus but eventually landed back by gravity to the horizontal wing (4.65 ms) and coalesced with an existing condensate drop (4.7 ms). The vapor condensation was discontinued soon afterward, and the particle-laden drop evaporated to become the displaced particle cluster in the center of Fig. 5*D*. The jumping process in Fig. 5*E* appeared similar to the floating removal process in Fig. 2.

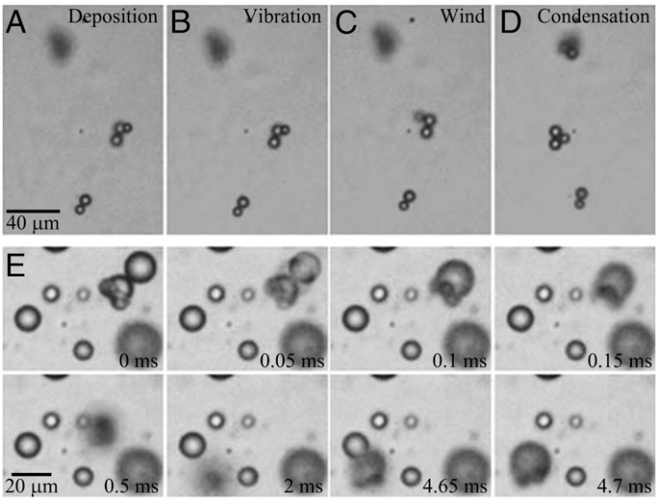


**Fig. 5.** Comparison of particle removal mechanisms. (*A*) Polystyrene particles 8 μm in diameter were initially dispersed on a cicada wing. (*B*) The particles could not be removed with mechanical vibration. (*C*) The particles could not be removed by airflow. (*D*) When the wing was exposed to condensing water vapor, the particles stuck after step *C* were dislodged by the self-propelled jumping condensate. Note that both the particles in the center and the particles on the top (out of focus because of the uneven wing) were dislodged by the jumping condensate. (*E*) The process for coalescence-induced dislodging of particles on a horizontally held cicada wing. A dew drop formed around an aggregate of three particles. This drop coalesced with an approaching dew drop, and the merged drop jumped off the wing (and therefore went out of focus). The particle-laden drop eventually landed back by gravity and coalesced with another drop on the horizontal wing. The motion of the relatively hydrophobic particles on the drop surface is apparent in Movie S4.

**Self-Cleaning of Biologically Relevant Contaminants.** To demonstrate the self-cleaning capability by the jumping condensate, we used pollen and silica particles to represent contamination of biological and inorganic origins, respectively (11). Before jumping, the solid particles could be slightly rotated and/or displaced by the accumulation of the condensate and the capillary forces associated with the rise in the liquid–gas interface. The rotation was shown by the position of the pollen particle in the first two images of Fig. 6*A* and the displacement by the bottom two silica particles in Fig. 6*B*. In Fig. 6*A*, a single pollen particle ~20 μm in diameter was removed from the wing by the jumping condensate. The jumping process was triggered by the coalescence of the drop encapsulating the particle with the surrounding condensate drops, similar to the lifting removal process in Fig. 3. In Fig. 6*B*, silica particles with an average diameter of 20 μm were initially dispersed on a cicada wing. As water condensate continued to nucleate around the silica particles, a group of particles suddenly merged and jumped away from the surface. Judging from the limited accumulation of condensate water, the jumping process in

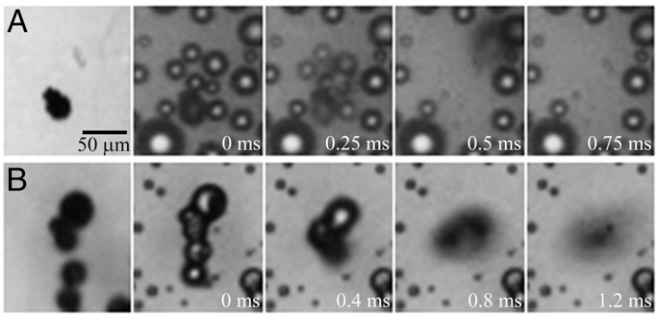


**Fig. 6.** Self-cleaning by the jumping condensate on horizontally held cicada wings. (*A*) Removal of a single pollen particle after coalescence with neighboring drops (Movie S5). (*B*) Removal of multiple silica particles upon coalescence (Movie S6).

Fig. 6*B* was likely related to the aggregating removal process in Fig. 4.

In Figs. 5 and 6, the wings were oriented horizontally to facilitate the experiments, which was why the dislodged particles eventually landed back on the wing. In reality, cicada wings are more likely to orient vertically as shown in Fig. 1*A*, in which case gravity will help to completely remove the contaminants from vertical or slanted surfaces. Even if the wing is oriented horizontally, the contaminants can still be driven off the wing surface by a series of cascading coalescences (5) or by the ambient airflow around the wing. In the latter case, the jumping condensate provides enough momentum for the contaminants to move out of the thin viscous boundary layer for airflow removal to become effective, much like the ballistospore discharge (19, 20). We experimentally confirmed that the jumping drops can accomplish self-cleaning regardless of the orientation of the wing.

In addition to the jumping-condensate cleaning mechanism, other possible mechanisms for removing contaminants include wind, gravity, vibration, and rain fall. Wind, gravity, and vibration were experimentally proved to be ineffective in removing small particles (Fig. 5), which is understandable from their unfavorable $R_p^2$ or $R_p^3$ scaling. However, wind and gravity can both augment the jumping-condensate removal mechanism, because both are more effective once the contaminants are free from the adhesive forces of the surface. Rainfall can be very effective in removing contaminants because rain drops carry a large momentum and water has a much higher viscosity than air. However, rainfall is unlikely to be acting alone for self-cleaning because it is less common than condensation, which takes place in humid weather on a daily basis.

## Discussion

With the jumping condensate, we demonstrated effective removal of organic and inorganic particles of a variety of wettabilities and sizes. The jumping-condensate removal mechanism has effectively removed particles with a diameter as large as 100 μm. Although larger particles can also be removed by the jumping condensate, accumulation of the condensate may take an impractically long time and, more importantly, other mechanisms such as gravity and vibration become increasingly effective beyond this scale. Due to the difficulty of high-speed imaging, we have demonstrated self-cleaning of particles only down to 8 μm. However, as a consequence of the favorable scaling with respect to the particle radius, the jumping-condensate removal mechanism is expected to work for particles with diameters down to the size of the surface roughness (order of 100 nm for cicada wings). Note that for superhydrophobic surfaces with a microscale roughness in addition to nanoscale topography, such as the lotus leaves with hierarchical structures, the microscale roughness may interfere with the self-cleaning by occasionally trapping particles within the microasperities (3, 26).

The jumping-condensate processes are expected to enable self-cleaning on most superhydrophobic surfaces. Compared with the conventional rolling removal mechanism (1), the jumping removal requires anti-dew superhydrophobicity (4, 27). Although the exact mechanism for dew repellency is still under research, most natural water-repellent surfaces are anti-dew. Synthetic superhydrophobic surfaces should also be anti-dew to be of practical use in natural environments, and the anti-dew property has already been demonstrated with properly designed (biomimetic) nanostructures. Indeed, the jumping phenomenon has been reported on a variety of natural surfaces including lotus leaves, lacewings, and springtails (28–30) as well as on synthetic superhydrophobic surfaces such as nanotextured silicon, aluminum, and copper (31–33). Note that the nanostructures (particularly the conical protuberances in Fig. 1*B*) also minimize the contact area and therefore adhesive forces between the particle and the superhydrophobic surface (11, 13), which is corroborated by the small contact angle hysteresis associated with fine textures (34–36). As a proof of concept, the jumping-condensate self-cleaning was achieved on nanostructured copper surfaces prepared following ref. 37 (Movie S7), suggesting new avenues for the development of self-cleaning materials.

## Conclusions

Using the cicada wing as a model surface, we have demonstrated that the self-propelled jumping condensate on superhydrophobic surfaces is an effective mechanism for removing a variety of contaminants, including both hydrophobic/hydrophilic and organic/inorganic particles. Compared with other removal mechanisms such as wind, gravity, and vibration, the jumping-condensate mechanism scales much more favorably for removing small-scale contaminants held by van der Waals and/or capillary bridging attractions and is particularly useful when rainfall is absent for an extended period. Our findings point to an alternative route to achieve autonomous self-cleaning, which is fundamentally different from the conventional wisdom requiring rolling and/or impacting droplets on the superhydrophobic surfaces.

## Materials and Methods

**Cicada Wings.** The cicadas, *P. claripennis*, were collected during summer in the greater Brisbane area in Queensland, Australia. The wings were surgically separated by a scalpel. For self-cleaning experiments, the forewings were cut into two equally sized pieces and attached by adhesive tape to a flat silicon or glass substrate. For atomic force microscope (AFM) imaging, the forewings were cut into smaller sections (*ca.* 3 × 5 mm) and epoxied to AFM mounted stubs. For the study of particle removal processes in Figs. 2–4 only, the wing sample was folded in the center to form a slender ridge on which the imaging system was focused; the main purpose was to prevent condensate drops far away from the imaging plane from interfering with the video microscopy. The ridge was ∼2 mm wide and ∼1 mm above the average wing surface. Care was taken to gently fold the wing to avoid altering its surface properties.

**Contaminant Particles.** For the study of particle removal processes, large particles were used: silver-coated solid glass spheres with a diameter range of 43–62 μm (Cospheric SLGMS-AG) and PMMA spheres with a diameter range of 90–106 μm (Cospheric PMPMS). For the demonstration of self-cleaning, synthetic particles were either silica beads with an average diameter of 20 μm (Kobo MSS-500/20) or fluorescent polystyrene divinylbenzene particles with a diameter of 8 μm (Thermo Scientific Fluoro-Max 35–3), representing hydrophilic and hydrophobic particles, respectively. Pollen particles were harvested from *Acacia cornigera* at the Duke University Research Greenhouses in Durham, NC.

**Imaging Methods.** AFM imaging was carried out with a ThermoMicroscope TMX-2000 Explorer. For side-view imaging of the jumping-condensate processes, an Infinity K2 microscope was used with a 10× Nikon objective. For top-view imaging of the self-cleaning processes, a Nikon LV150 microscope

was used with a 10× or 20× lens. The movies were captured by a Phantom v7.1 or v710 camera with up to 60,000 frames per second (fps), sometimes with a 0.7× demagnification lens for larger fields of view.

**Vapor Condensation.** Condensation of water vapor was induced either by placing the wings on a cold plate chilled below the dew point of the ambient air, or by directing toward the wing saturated vapor flow that was generated using a heated porous wick soaked with water (or simply a household ultrasonic humidifier). Care was taken to avoid imposing strong vapor flow directly on the wing. These two methods simulated condensation processes in still air and misty breezes, respectively. The condensation processes were comparable in both cases.

**Mechanical Vibration.** Mechanical vibration was produced by a wave driver (Pasco SF-9324) for 30 s. The frequency of vibration was set at 22 Hz, which was calculated using the frequency–mass relationship for flying insects (24), assuming an average cicada mass of 2.25 g. The maximum speed of vibration was measured with the aforementioned video imaging system.

**Wind Flow.** The miniwind tunnel was custom built with a cross-section area of 30 × 30 cm. A rotary fan produced an airflow with an average free-stream speed of up to 12 m/s, which was measured by an anemometer (CFM Master II). Airflows of 30 s, 60 s, and 90 s were tested, verifying that the duration of exposure to the wind flow did not affect the particle removal by wind.

**ACKNOWLEDGMENTS.** We thank J. Boreyko, J. Feng, and G. Ghigliotti for helpful discussions, N. Bumb and P. McGuire for constructing the wind tunnel, and M. Barnes and J. Gordon for providing the pollen particles. K.M.W. was supported by Duke University's Pratt Fellows Program administrated by M. Absher. This project was supported in part by the James Cook University Faculty Administered Internal Grant (to G.S.W.) and by the Defense Advanced Research Projects Agency, Intel Corporation, the National Science Foundation, and the North Carolina Space Grant (to C.-H.C.).

1. Barthlott W, Neinhuis C (1997) Purity of the sacred lotus, or escape from contamination in biological surfaces. *Planta* 202:1–8.
2. Blossey R (2003) Self-cleaning surfaces—virtual realities. *Nat Mater* 2(5):301–306.
3. Fürstner R, Barthlott W, Neinhuis C, Walzel P (2005) Wetting and self-cleaning properties of artificial superhydrophobic surfaces. *Langmuir* 21(3):956–961.
4. Quéré D (2005) Non-sticking drops. *Rep Prog Phys* 68:2495–2532.
5. Boreyko JB, Chen CH (2009) Self-propelled dropwise condensate on superhydrophobic surfaces. *Phys Rev Lett* 103(18):184501.
6. Boreyko JB, Chen CH (2010) Self-propelled jumping drops on superhydrophobic surfaces. *Phys Fluids* 22:091110.
7. Visser J (1995) Particle adhesion and removal: A review. *Particul Sci Technol* 13(3–4): 169–196.
8. Israelachvili J (2011) *Intermolecular and Surface Forces* (Academic, Amsterdam), 3rd Ed.
9. Butt H, Kappl M (2010) *Surface and Interfacial Forces* (Wiley-VCH, Weinheim, Germany).
10. Wagner T, Neinhuis C, Barthlott W (1996) Wettability and contaminability of insect wings as a function of their surface sculptures. *Acta Zool* 77:213–225.
11. Hu HM, Watson JA, Cribb BW, Watson GS (2011) Fouling of nanostructured insect cuticle: Adhesion of natural and artificial contaminants. *Biofouling* 27(10):1125–1137.
12. Azuma A (1992) *The Biokinetics of Flying and Swimming* (Springer, Tokyo).
13. Watson GS, Myhra S, Cribb BW, Watson JA (2008) Putative functions and functional efficiency of ordered cuticular nanoarrays on insect wings. *Biophys J* 94(8):3352–3360.
14. Min W, Jiang B, Jiang P (2008) Bioinspired self-cleaning antireflection coatings. *Adv Mater* 20:3914–3918.
15. Binks B, Horozov T, eds (2006) *Colloidal Particles at Liquid Interfaces* (Cambridge Univ Press, Cambridge, UK).
16. Leenaars A (1989) *Particles on Surfaces 1*, ed Mittal K (Plenum, New York), pp 361–372.
17. O'Brien S, van den Brule B (1991) A mathematical model for the cleansing of silicon substrates by fluid immersion. *J Colloid Interface Sci* 144:210–221.
18. Kralchevsky PA, Nagayama K (2000) Capillary interactions between particles bound to interfaces, liquid films and biomembranes. *Adv Colloid Interface Sci* 85(2–3):145–192.
19. Pringle A, Patek SN, Fischer M, Stolze J, Money NP (2005) The captured launch of a ballistospore. *Mycologia* 97(4):866–871.
20. Noblin X, Yang S, Dumais J (2009) Surface tension propulsion of fungal spores. *J Exp Biol* 212(17):2835–2843.
21. Rykaczewski K, et al. (2011) Three dimensional aspects of droplet coalescence during dropwise condensation on superhydrophobic surfaces. *Soft Matt* 7:8749–8752.
22. Buller A (1909) *Researches on Fungi* (Longmans, Green, London), Vol 1.
23. Ducker W, Xu Z, Israelachvili J (1994) Measurements of hydrophobic and DLVO forces in bubble-surface interactions in aqueous solutions. *Langmuir* 10:3279–3289.
24. Park J, Yoon K (2009) *Intelligent Unmanned Systems: Theory and Applications*, eds Budiyono A, Riyanto B, Joelianto E (Springer, Berlin), pp 119–133.
25. Meissner T, Smith D, Wentz F (2001) A 10 year intercomparison between collocated special sensor microwave imager oceanic surface wind speed retrievals and global analyses. *J Geophys Res* 106:11731–11742.
26. Bhushan B, Jung YC, Koch K (2009) Self-cleaning efficiency of artificial superhydrophobic surfaces. *Langmuir* 25(5):3240–3248.
27. Boreyko JB, Chen CH (2009) Restoring superhydrophobicity of lotus leaves with vibration-induced dewetting. *Phys Rev Lett* 103(17):174502.
28. Mockenhaupt B, Ensikat HJ, Spaeth M, Barthlott W (2008) Superhydrophobicity of biological and technical surfaces under moisture condensation: Stability in relation to surface structure. *Langmuir* 24(23):13591–13597.
29. Watson JA, Cribb BW, Hu HM, Watson GS (2011) A dual layer hair array of the brown lacewing: Repelling water at different length scales. *Biophys J* 100(4):1149–1155.
30. Helbig R, Nickerl J, Neinhuis C, Werner C (2011) Smart skin patterns protect springtails. *PLoS ONE* 6(9):e25105.
31. Chen X, et al. (2011) Nanograssed micropyramidal architectures for continuous dropwise condensation. *Adv Funct Mater* 21:4617–4623.
32. He M, et al. (2012) Hierarchically structured porous aluminum surfaces for high-efficient removal of condensed water. *Soft Matt* 8:6680–6683.
33. Miljkovic N, et al. (2013) Jumping-droplet-enhanced condensation on scalable superhydrophobic nanostructured surfaces. *Nano Lett* 13(1):179–187.
34. Reyssat M, Quéré D (2009) Contact angle hysteresis generated by strong dilute defects. *J Phys Chem B* 113(12):3906–3909.
35. Dorrer C, Rühe J (2011) Micro to nano: Surface size scale and superhydrophobicity. *Beilstein J Nanotechnol* 2:327–332.
36. Koishi T, Yasuoka K, Fujikawa S, Zeng XC (2011) Measurement of contact-angle hysteresis for droplets on nanopillared surface and in the Cassie and Wenzel states: a molecular dynamics simulation study. *ACS Nano* 5(9):6834–6842.
37. Boreyko JB, Zhao Y, Chen CH (2011) Planar jumping-drop thermal diodes. *Appl Phys Lett* 99:234105.